COADS as a Diagnostic Modeling Tool: Air-Sea Interaction and the Role of the Deep Ocean in Climate Change

Howard P. Hanson
Atmospheric and Climate Dynamics Program
Cooperative Institute for Research in Environmental Sciences
University of Colorado at Boulder 80309-0216

Summary

The availability of the Comprehensive Ocean-Atmosphere Data Set (COADS) has provided the climate research community with a powerful tool for the study of climate variability and change. As seen in the papers in this volume, Release 1 of the COADS contains a variety of instrumental and other uncertainties, all of which make sensitive analyses using this release difficult. With the newer, more controlled and complete release of the COADS will come the additional capability of merging the data with physical models of various climate processes. This contribution illustrates one such use of the COADS as a diagnostic modeling tool by using turbulent fluxes and other quantities derived from Release 1 and its Interim Release to infer regions of the North Atlantic that could be particularly susceptible to climate change.

1. Introduction

One of the most compelling problems that climate researchers face today is the role of anthropogenically-induced radiatively-active trace gases in the climate system. These "greenhouse gases," which are transparent to sunlight but relatively opaque to longwave radiation, have the potential to warm the climate by altering the planetary radiation balance. Whether or not other processes in the climate system will be able to counteract this potential for warming is a topic of intense research. Because the time scales over which this warming could occur are in the range of decades to centuries, long-term climatological records such as the COADS are particularly valuable.

The time scales of relevance for global warming are associated mainly with two factors: the rate of increase of the greenhouse gases in the atmosphere and the storage, transport, and release of heat by the ocean. The oceanic "flywheel," which determines the latter of these factors, influences both the storage and release of heat as well as the ocean's chemical buffering capacity. Atmospheric concentrations of greenhouse gases that are soluble in seawater, such as CO, are profoundly affected by this buffering. To the extent that climate change could change the ocean's heat storage and buffering abilities, a feedback between the ocean circulation and climate exists, one that is not at all well understood.

The processes that are most important in this feedback are the *vertical mixing* of heat, salt, and chemicals into the seasonal and main thermoclines. The depth to which this mixing extends determines, in part, the time scales mentioned above. This depth, in turn, depends strongly on air-sea interaction processes.

The two main large-scale circulation systems in the ocean that are associated with deep mixing are the thermohaline circulation, the global “conveyer belt” that includes all of the ocean basins, (Broecker, 1992) and thermocline ventilation, (Luyten et al., 1983) via subduction in the wind-driven gyres in each separate ocean basin. Mixing in the turbulent boundary layer of the ocean-in the oceanic mixed layer-is important in both of these circulation systems. The annual cycle of the mixed layer (deep and cold in winter; shallow and warm in summer) acts to inject water that has been in contact with the atmosphere into the sub-surface components of these two large-scale circulation systems, and therefore the processes that control the annual cycle of the mixed layer are an important component of the climate system.

This contribution is concerned with investigating the behavior of the annual cycle of the mixed layer of the North Atlantic by using the COADS as the basis for a diagnostic modeling study. In addition to providing insight into the effect of mixed layer processes on the larger scale circulations of the ocean, this study illustrates the potential of the COADS when used in non-traditional modes.

2. Background

The oceanic mixed layer, which varies in depth from less than 20 m in the doldrums during summer to the entire water column at times in the northern convective regions, is a result of turbulent mixing that is forced by mechanical mixing due to the wind stress and by buoyancy forces associated with surface fluxes

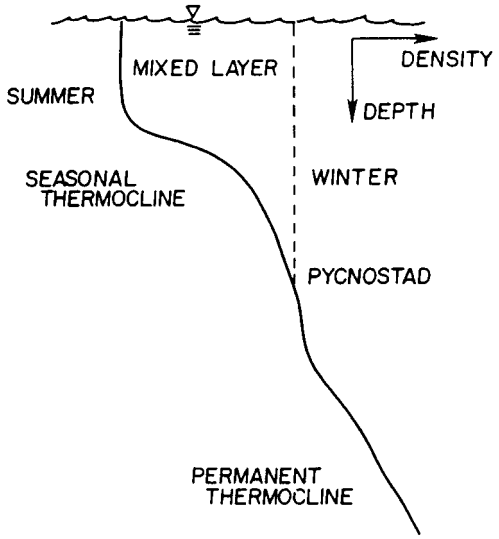

Fig. 1 Schematic diagram of the oceanic mixed layer, presented in terms of the density profile. The shallow summer mixed layer (solid) deepens and cools to heavier, more dense water to a wintertime layer (dashed) and, in the process, erodes the seasonal thermocline. In the spring, the deep layer retreats and leaves behind a new year’s seasonal thermocline as it warms to the less dense, shallow layer of the next summer.

of heat and water. The basic theory of the mixed layer model was formulated some 25 years ago by Kraus and Turner, 1967 and is based on ideas originally presented by Ball, 1961. Although there has been a large body of work on the topic since the basic theory was published, a useful tutorial that is still reasonably complete is contained in the chapter by Niiler and Kraus, 1977.

The fundamental assumption in mixed-layer models is that vertical mixing by turbulence is sufficiently strong to eliminate vertical gradients of the horizontally-averaged state variables. This assumption is surprisingly valid over most of the world's ocean. It implies that the vertical profiles of temperature, salinity, and momentum, as well as other trace chemicals, are constant between the surface and some depth-the mixed layer depth. Figure 1 presents an idealized schematic of summer (solid) and winter (dashed) mixed layers from the perspective of the density profile.

It is control of the mixed-layer depth by air-sea interaction processes that is of interest here. In physical terms, the mixed-layer model is derived from the principle that sources of turbulence kinetic energy (TKE) are balanced by dissipation and conversion to potential energy. The latter, associated with lifting relatively heavy water from the thermocline into the mixed layer, is associated with turbulent entrainment across the base of the mixed layer when sources of TKE are strong. On the other hand, when TKE sources are weak, such as at times and places where there is surface heating by strong solar radiation absorption, entrainment in deep mixed layers cannot be maintained, and an adjustment to a new, warm and shallow, layer occurs. When this happens, the water that was previously in the deeper, colder mixed layer remains in the thermocline, where it is swept into the larger scale circulation systems.

The mixed-layer model formalism uses a vertical integral of the TKE equation and a parameterization of turbulent dissipation (which is taken to be proportional to TKE sources) to relate TKE sources and dissipation to potential energy conversion via entrainment. Sources include mechanical mixing by the wind, which can be shown to be related to the friction velocity $u.*$, and buoyancy fluxes, which, if positive (upward) create heavy water parcels at the surface that sink, creating TKE. The surface buoyancy flux B is a combination of heat and salinity fluxes:

$$B = \frac{g}{Q}\left[\frac{\alpha}{c}(H + LE + R) + \beta S(E + P)\right] \qquad (1)$$

where g, c, and L are gravitational acceleration, the specific heat of seawater, and the latent heat of condensation, respectively; ρ, (α, and β are the density of seawater and its thermal expansion and haline contraction coefficients, respectively; and the surface fluxes of sensible heat, water (evaporation), net radiation, and precipitation are given respectively by H, E, R, and P (all are defined here to be positive in the upward direction, so that $P<O$ always and the solar component of R is also negative). Because B can be either positive (a source of turbulence) or, when heating and precipitation dominate, negative (and thus a sink of turbulence, because light parcels have to be mixed downward), the dissipation parameterization involves a rectifying formulation:

$$\widehat{B} \equiv \frac{1}{2}[(B - |B|) + n(B + |B|)] \qquad (2)$$

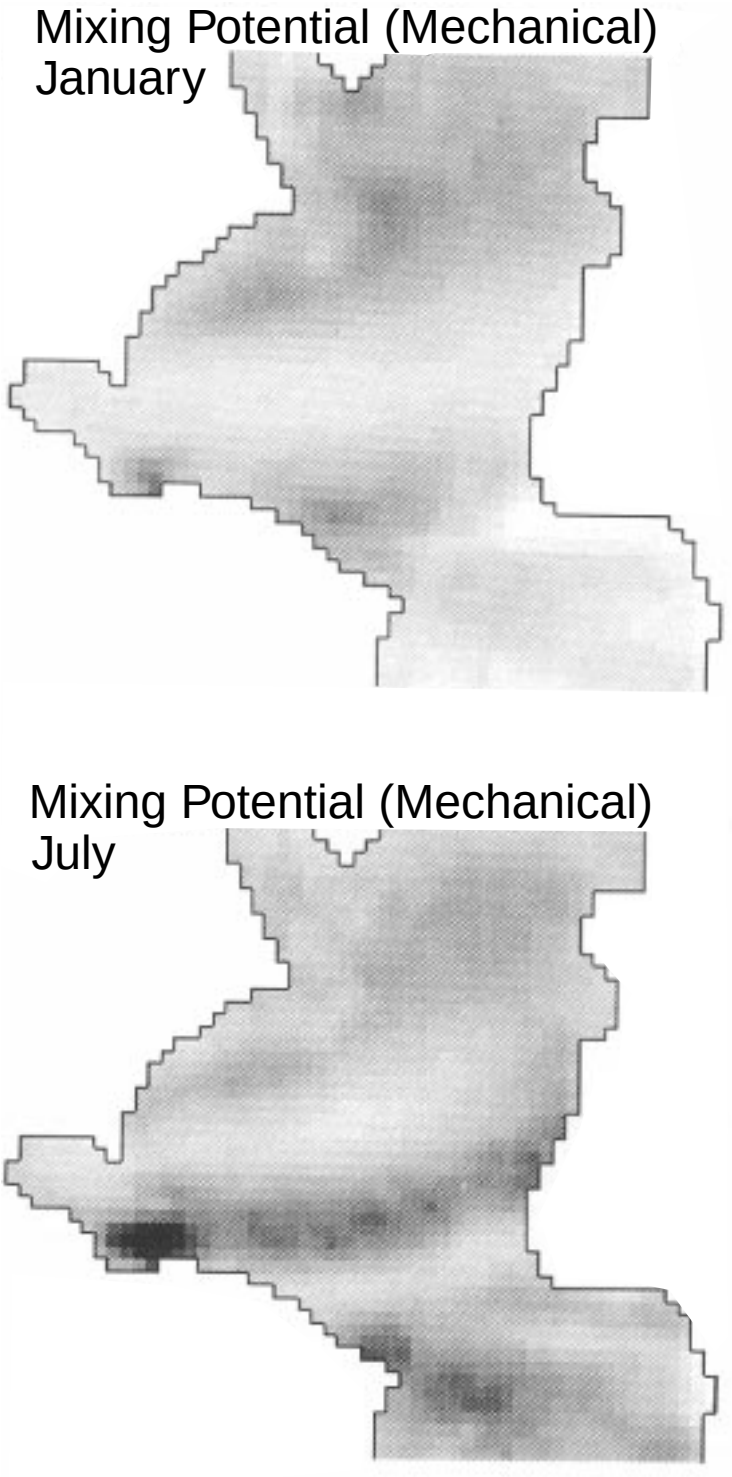

Figure 2. Mechanical mixing potential, that is, the mixing potential associated with wind stirring, for the North and Tropical Atlantic for January (top) and July (bottom). Darker shades indicate stronger mixing potential: it will be noted that the mechanical mixing is never as strong as mixing due to buoyancy forces (fig. 3).

When $B>O$, implying that the ocean is losing buoyancy, this is nB, and the amount $(1-n)B$ is the dissipation of buoyantly generated TKE. Estimates of n in the ocean center around 0.3. The mechanical source of TKE-due to the physical stirring of the water by the wind, is parameterized proportionately to the friction velocity as $mu*/h$, where h is the mixed-layer depth and m encompasses both the wind-mixing efficiency and its dissipation, and the conversion of TKE to potential energy is simply $w_e\Delta b/h$, the entrainment rate (specified as a velocity) times the buoyancy jump across the mixed-layer base divided by the mixed layer depth. In the mixed-layer model, the time- dependence of the mixed-layer depth is simply the integral of w_e (with whatever corrections are relevant for large-scale vertical motion). For the purpose of this study, it is sufficient to examine only the potential energy conversion in this form. This can be defined as a mixing potential:

$$M = \frac{w_e \Delta b}{h} = \frac{mu*^3}{\quad} + \hat{B} \geq 0 \qquad (3)$$

with the important caveat that, since there can be no "unmixing," $M \geq 0$. In physical terms, the mixing potential is the amount of energy available to entrain dense water from the thermocline into the mixed layer. Note that it is possible to partition M into a mechanical mixing component [the first term in (3)], and, using (1), components due to turbulent mixing and the radiation and precipitation. This is a useful separation because the turbulent components are associated with strong feedback between ocean and atmosphere, since these fluxes involve the air-sea temperature difference.

Given estimates of h and the radiation and precipitation, the COADS can now be used to derive $u*$ and the turbulent fluxes of sensible and latent heat, providing estimates of M without the direct use of an ocean circulation model. This is what is meant by using the COADS as a diagnostic modeling tool.

3. Results

The COADS Release 1 and the subsequent Interim Release were used to derive fields of $u*$ and the turbulent fluxes of sensible heat and evaporation for the North Atlantic basin between 60°N and 20°S. The individual monthly averages for the 30-year period 1959-1989 were averaged to develop a 30-year climatology for the basin. In calculating the friction velocity, evaporation, and sensible heat flux from the Release 1 variables, the product of the wind speed and sea-air temperature difference was multiplied by a calculated air density and a surface transfer coefficient based on the work of Smith, 1988. The period chosen provides quite good data coverage and reasonably good data homogeneity for the North Atlantic basin.

Radiation and precipitation data, for the results shown here, are zonally averaged, monthly data. The precipitation data were interpolated from the seasonal data presented by Dorman and Bourke 1981, and the radiation data, being one of the strongest components of M, were inferred from the COADS-derived total turbulent heat flux and the storage and transport data presented by Lamb and Bunker, 1982. This method uses the heat budget to deduce the radiative heating/cooling as a residual of the heat storage and transport and surface turbulent fluxes. It ensures that the radiative

fluxes used are self consistent with the observed climatology of the basin. Future studies are planned with zonally variable radiative fluxes and precipitation taken from the empirical formulae commonly used in climatological analyses, such as the Oberhube 1991 atlas.

The mixed-layer depth enters the calculation by modifying the mechanical mixing term, and the COADS does not contain this quantity either. For this study, values of h taken from the seasonal simulation discussed by Bleck et al., 1989, were zonally averaged and used in Eqn. (3). It will be noted that this term is substantially weaker than the buoyancy flux term, so the errors introduced by using this estimate are small.

a. Mechanical mixing potential

Although calculations were made for all 12 months, only representative results will be shown here, for brevity. Figure 2 presents the mechanical mixing term *mu*h* for January and July. This and subsequent figures use shading to indicate mixing potential with darkest shading showing strongest mixing potential. (The actual scale varies from 0 [lightest] to $50 \cdot 10^{-8} m^2 s^{-3}$ [darkest-which occurs in Figs 3 and 4]. Since buoyancy units are $m^2 s^{-2}$, this is simply the time rate of change of buoyancy, a physically reasonable measure of mixing).

The pattern of mechanical mixing potential reflects mainly the strength of the wind, with the relatively light winds over the Sargasso Sea under the Subtropical High being evident in both January and July. The trade wind belt is strengthened, particularly in July, just off the coast of Venezuela by a sea-breeze-like amplification, and the westerlies produce a higher mixing potential over most of the north part of the basin. The effect of seasonal variability of the mixed layer depth is evident in the somewhat larger mixing potential overall in July than in January: the mixed-layer depth changes more between the seasonal extremes than the wind speed.

b. Contribution of turbulent fluxes

The contribution of the turbulent fluxes of sensible and latent heat, including the effect of evaporation on the saline contribution to the buoyancy flux [see Eqn. (1)) is shown in Fig. 3. The same shading scale as in Fig. 2 is used here; this underscores the stronger contribution of the turbulent fluxes than the mechanical contribution.

Figure 3 is dominated by the patterns of sea-air temperature difference, with largest contributions associated with the Gulf Stream and North Atlantic Current. In winter, there are also significant contributions from the turbulent fluxes over the Labrador Sea and to the southeast of Greenland. The July patterns are significantly weaker, with the effect of warm air flowing over cold water off Nova Scotia producing a minimum in the mixing potential.

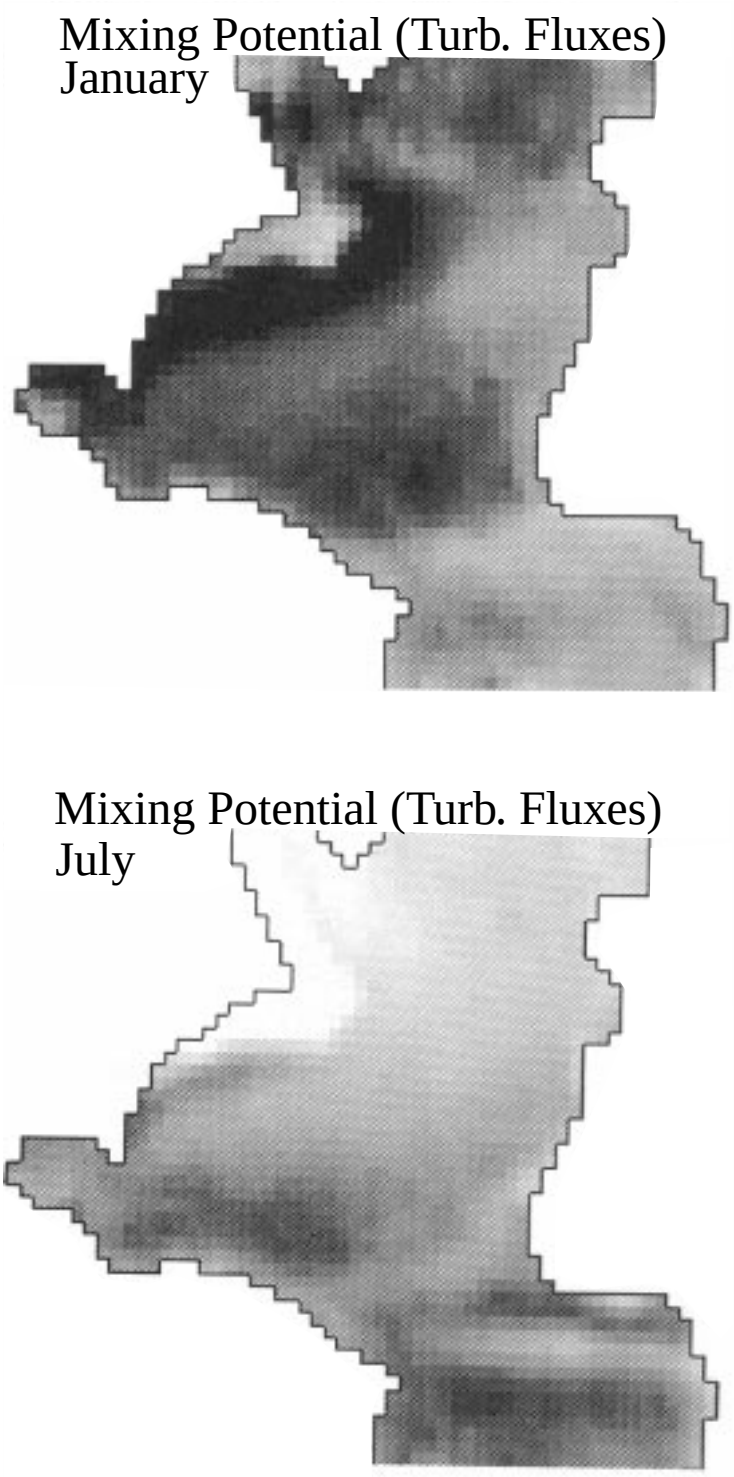

Figure 3. Mixing potential associated with turbulent fluxes (sensible and latent heat, as well as the effect of evaporation on the saline contribution to the buoyancy flux). Shading is on the same scale as Fig. 2; this makes obvious how much more effective buoyancy fluxes are in determining the mixing potential.

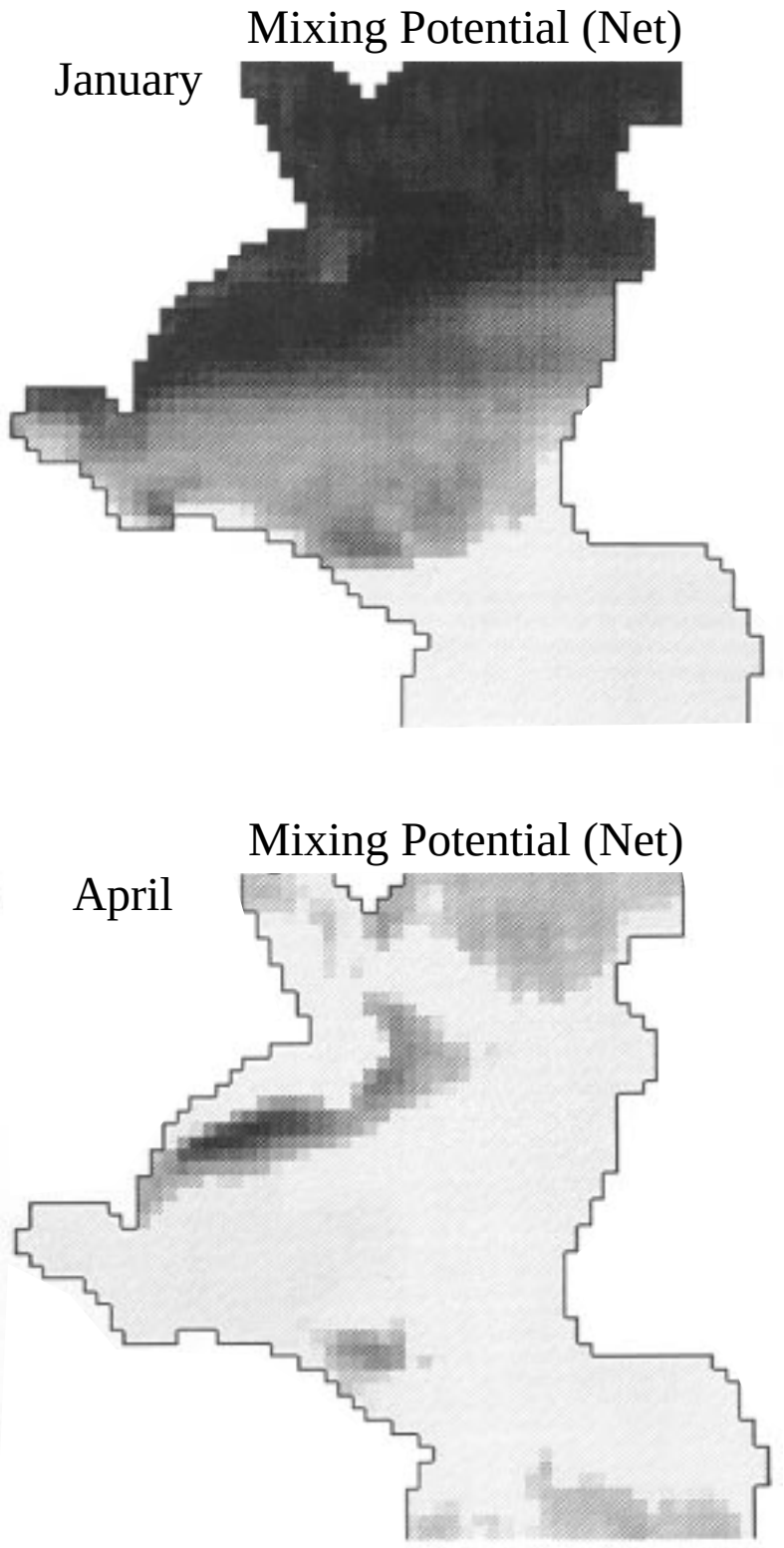

Figure 4. Net mixing potential, which combines the COADS-derived quantities in Figs. 2 and 3 with precipitation and radiative flux data as described in the text.

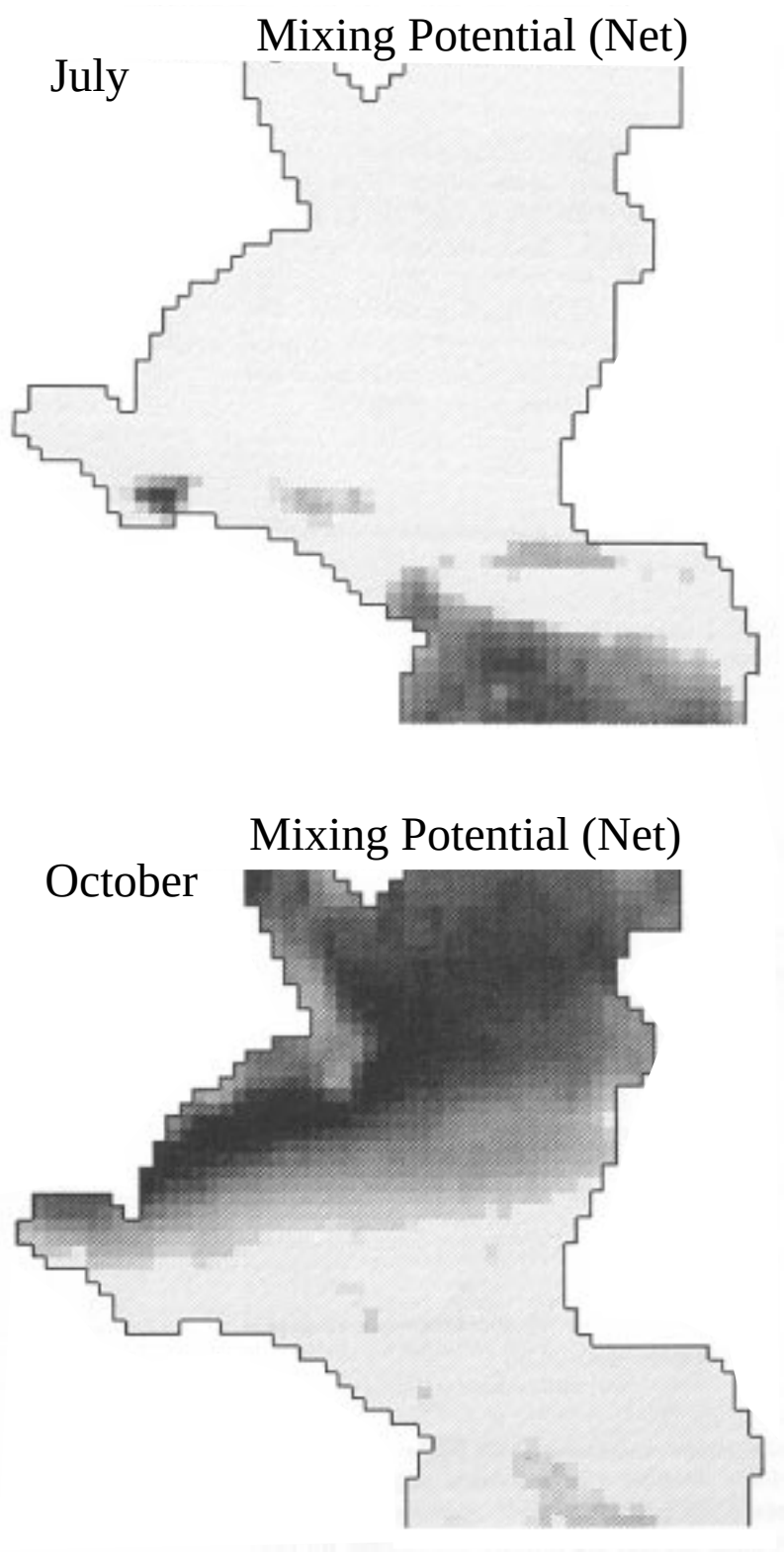

Figure 4(continued).

c. Net mixing potential

When the mechanical and turbulent contributions are combined with the radiative fluxes and precipitation (both of which are in zonally averaged form here), the net mixing potential shown in Fig. 4 results. Note that, in addition to the January and July maps, the net effect for April and October are also shown in Fig. 4. The annual cycle of net mixing potential for the North Atlantic is dominated by wintertime mixing over the Gulf Stream and the regions south of Greenland; this deep injection of surface properties begins in fall, as shown in the October map, and continues through April.

The July pattern, on the other hand, is dominated by the radiative fluxes, which cut off mixing over the entire North Atlantic basin in July. This has the effect of isolating the water masses in the seasonal thermocline during the boreal summer and allowing this water to become swept into the sub-surface circulation systems. Also, the mechanical contribution off the northwest coast of Venezuela is apparent in the net contribution.

4. Commentary

There are two relevant conclusions to be drawn from this example of using the COADS for diagnostic modeling. First, the thermohaline forcing of deep mixing in the North Atlantic is dominated by air-sea heat and moisture exchange over the Gulf Stream and the North Atlantic Current, with large areas near Greenland also being important. Although the extent to which these regions are directly responsible for deep and intermediate water production in the large-scale circulation systems of the basin can be quantified only with circulation models, the results presented here point to areas of particular sensitivity in these circulations.

Second, and from a more personal perspective, it seems appropriate to emphasize the importance of the resource provided by the COADS for a variety of research topics. In addition to this new diagnostic modeling approach, I have been able to use the dataset for studies of storm tracks, (Hanson et al., 1985) air-sea interaction climatologies, (Hanson et. al., 1991) and cloud-climate studies (Hanson, 1991). None of this work would have been possible without the COADS project. As the dataset matures, it can be reasonably expected that other, new and innovative climate-related research will be forthcoming. The continued support of this project is crucial to understanding Earth’s climate and its variability.

Acknowledgements

This contribution is a result of research supported by Grant No. DE-FG02-90ER61019 from the Carbon Dioxide Research Program, U.S. Department of Energy. I am pleased to acknowledge help from David Hoge with the graphical software used for the figures, and stimulating conversations with my Co-PI, Prof. Rainer Bleck of the University of Miami, that motivated the approach used in deriving the new results presented here. Scott Woodruff and Sandy Lubker deserve special recognition for their patient help with all of my COADS-related research over the past decade.

References

Ball, F.K., 1961: Control of inversion height by surface heating. *Quarterly Journal of the Royal Meteorological Society,* **86**, 483-494.

Bleck, R., Hanson, H.P., Hu, D., and Kraus, E.B., 1989: Mixed layer - thermocline interaction in a three-dimensional isopycnic coordinate model. *Journal of Physical Oceanography*, **19**, 1417-1439.

Broecker, W.S., 1992: The great ocean conveyer. Oceanography, 4,79-89.

Dorman, C.E., and Bourke, R.H., 1981: Precipitation over the Atlantic Ocean, 30°S to 70°N. *Monthly Weather Review*, **109**, 554563.

Hanson, H.P 1991: Marine stratocumulus climatologies. *International Journal of Climatology,* **11**, 147-164.

Hanson, H.P., and Long, B., 1985: Climatology of cyclogenesis over the East China Sea. *Monthly Weather Review,* **113**, 697-707.

Hanson, H.P., Cornillon, P., Halliwell, G.R., and Halliwell, V., 1991: Climatological perspectives, oceanographic and meteorological, on variability in the Northeast Atlantic. *Journal of Geophysical Research*, **96**, 8517-8529.

Kraus, E.B., and Turner, J.S., 1967: A one-dimensional model of the seasonal thermocline. Part 11: The general theory and its consequences. *Tellus*, **19**, 98- 106.

Lamb, P.J., and Bunker, A.J., 1982: The annual march of the heat budget of the North and Tropical Atlantic Ocean. *Journal of Physical Oceanography*, **12**, 1388-1410.

Luyten, J.R., Pedlosky, J., and Stommel, H., 1983: The ventilated thermocline. *Journal of Physical Oceanography,* **13**, 292-309.

Niiler, P.P., and Kraus, E.B., 1977: One-dimensional models of the upper ocean. In: *Modelling and Prediction of the Upper Layers of the Ocean*, E.B. Kraus, (ed.), Pergamon Press, 143172.

Oberhuber, J.M., 1991: *An Atlas Based on the COADS Dataset*. Max Plank Institute, Rep. 15.

Smith, S.D., 1988: Coefficients for sea surface wind stress, heat flux, and wind profiles as a function of wind speed and temperature. *Journal of Geophysical Research*, **93**, 15467-15472.